

## Copper Corroles Are Inherently Saddled

Abraham B. Alemayehu, Emmanuel Gonzalez, Lars Kristian Hansen, and Abhik Ghosh\*

Department of Chemistry and Center for Theoretical and Computational Chemistry, University of Tromsø, 9037 Tromsø, Norway

Received April 17, 2009

X-ray crystallographic analyses of two sterically unhindered copper *meso*-triarylcorroles, Cu[5,15-P<sub>2</sub>-10-(4-MeOP)C] and Cu[5,15-(4-CF<sub>3</sub>P)<sub>2</sub>-10-(4-MeOP)C] (P = phenyl and C = corrole), revealed substantially saddled corrole rings. These results are in marked contrast to those on highly sterically hindered cobalt(III) and iridium(III) corroles, which exhibit planar corrole macrocycles. The solution to this conundrum is that copper corroles are inherently saddled, as a result of a specific copper(d)–corrole( $\pi$ ) orbital interaction. This orbital interaction results in a noninnocent corrole ligand, and the overall electronic structure may thus be described as Cu<sup>II</sup>–corrole<sup>\*2-</sup>. While many specific metal(d)–macrocycle( $\pi$ ) orbital interactions are known for nonplanar metalloporphyrins, this work provides a rare example of such an orbital interaction providing the actual driving force for a significant nonplanar distortion. Our findings on copper corroles, along with those of others on cobalt and iridium corroles, thus constitute an intriguing and somewhat counterintuitive chapter in the structural chemistry of metallocorroles.

### Introduction

Ever since the development of convenient one-pot syntheses of corroles by the Gross and Paolesse groups,<sup>1,2</sup> the chemistry of corroles has grown at an almost explosive pace.<sup>3,4</sup> Indeed, except in the biological arena (where hemes are all-important), it would not be an exaggeration to say that the chemistry of corroles has begun to rival that of porphyrins.<sup>3,4</sup> Corroles have found many applications, as catalysts of synthetic transformations, as nonlinear optical materials, and as photovoltaics, to give just a few examples.<sup>3,5,6</sup> In our laboratory, we have studied substituent effects in various metallocorroles by means of electronic absorption spectroscopy and electrochemistry and found the electronic spectra of copper corroles to be exceptionally sensitive to peripheral

substituents.<sup>7–9</sup> Thus, for the copper triarylcorroles [these being formally copper(III) species] that we have studied, the Soret maximum spans a range of 100 nm.<sup>10</sup> To analyze these remarkable electronic effects, in particular to dissect the effects of the 5,15- and 10-substituents, we synthesized a family of *meso*-A<sub>2</sub>B-triarylcorroles. Although the results of that study were interesting in their own right (and will be reported in due course), the most intriguing finding turned out to be the novel geometrical features of two of the complexes — Cu[5,15-P<sub>2</sub>-10-(4-MeOP)C] and Cu[5,15-(4-CF<sub>3</sub>P)<sub>2</sub>-10-(4-MeOP)C] (P = phenyl and C = corrole; Figure 1) — which lent themselves to X-ray crystallographic analysis. It is these structural features that we discuss in depth in this paper; we will compare them with other metallocorroles and attempt to understand the overall structural chemistry with the help of density functional theory (DFT) calculations.<sup>11,12</sup>

\*To whom correspondence should be addressed. Email: abhik@chem.uit.no.

(1) (a) Gross, Z.; Galili, N.; Saltsman, I. *Angew. Chem., Int. Ed.* **1999**, *38*, 1427–1429. (b) Paolesse, R.; Mini, S.; Sagone, F.; Boschi, T.; Jaquinod, L.; Nurco, D. J.; Smith, K. M. *Chem. Commun.* **1999**, 1307–1308. (c) Koszarna, B.; Gryko, D. T. *J. Org. Chem.* **2006**, *71*, 3707–3717.

(2) (a) Ghosh, A. *Angew. Chem., Int. Ed.* **2004**, *43*, 1918–1931. (b) Gryko, D. T. *Eur. J. Inorg. Chem.* **2002**, 1735–1743.

(3) Aviv, I.; Gross, Z. *Chem. Commun.* **2007**, 1987–1999.

(4) Gross, Z.; Gray, H. B. *Comments Inorg. Chem.* **2006**, *27*, 61–72.

(5) Albert, I. D. L.; Marks, T. J.; Ratner, M. A. *Chem. Mater.* **1998**, *10*, 753–762.

(6) Misra, R.; Kumar, R.; PrabhuRaja, V.; Chandrashekar, T. K. *J. Photochem. Photobiol. A* **2005**, *175*, 108–117.

(7) (a) Steene, E.; Wondimagegn, T.; Ghosh, A. *J. Phys. Chem. B* **2001**, *105*, 11406–11413. (b) Addition and Correction: *J. Phys. Chem. B* **2002**, *106*, 5312–5312.

(8) Wasbotten, I. H.; Wondimagegn, T.; Ghosh, A. *J. Am. Chem. Soc.* **2002**, *124*, 8104–8116.

(9) Steene, E.; Wondimagegn, T.; Ghosh, A. *J. Am. Chem. Soc.* **2003**, *125*, 16300–16309.

(10) (a) Thomas, K. E.; Wasbotten, I. H.; Ghosh, A. *Inorg. Chem.* **2008**, *47*, 10469–10478. (b) Addition and Correction: Thomas, K. E.; Wasbotten, I. H.; Ghosh, A. *Inorg. Chem.* **2009**, *48*, 1257–1257.

(11) Reviews on DFT studies of porphyrins and related compounds: (a) Ghosh, A. *Acc. Chem. Res.* **1998**, *31*, 189–198. (b) Ghosh, A. In *The Porphyrin Handbook*; Kadish, K. M., Guillard, R., Smith, K. M., Eds.; Academic: San Diego, CA, 1999; Vol. 7; Chapter 47, pp 1–38. (c) Ghosh, A.; Steene, E. *J. Biol. Inorg. Chem.* **2001**, *6*, 739–752. (d) Ghosh, A. *J. Biol. Inorg. Chem.* **2006**, *11*, 712–724.

(12) DFT studies of corroles and corrole analogues: (a) Ghosh, A.; Jynge, K. *Chem. Eur. J.* **1997**, *3*, 823–833. (b) Ghosh, A.; Wondimagegn, T.; Parusel, A. B. *J. Am. Chem. Soc.* **2000**, *122*, 5100–5104. (c) Bendix, J.; Dmochowski, I. J.; Gray, H. B.; Mahammed, A.; Simkhovich, L.; Gross, Z. *Angew. Chem., Int. Ed.* **2000**, *39*, 4048–4051. (d) Tangen, E.; Ghosh, A. *J. Am. Chem. Soc.* **2002**, *124*, 8117–8121. (e) van Oort, B.; Tangen, E.; Ghosh, A. *Eur. J. Inorg. Chem.* **2004**, 2442–2445. (f) Ghosh, A.; Wasbotten, I. H.; Davis, W.; Swarts, J. C. *Eur. J. Inorg. Chem.* **2005**, 4479–4485. (g) Wasbotten, I.; Ghosh, A. *Inorg. Chem.* **2006**, *45*, 4910–4913.

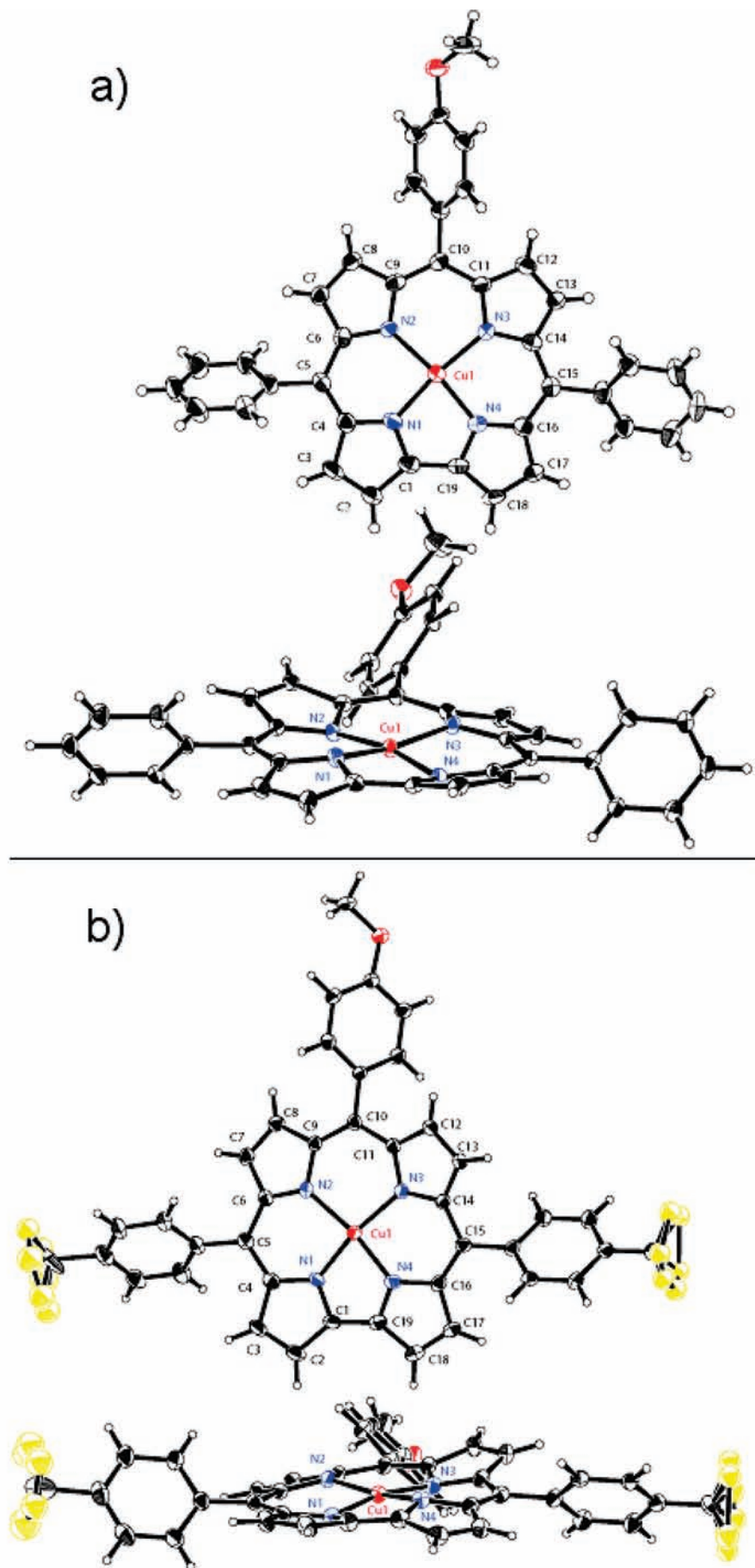


**Figure 1.** ORTEPs of (a)  $\text{Cu}[5,15\text{-P}_2\text{-}10\text{-}(4\text{-MeOP})\text{C}]$  and (b)  $\text{Cu}[5,15\text{-}(4\text{-CF}_3\text{P})_2\text{-}10\text{-}(4\text{-MeOP})\text{C}]$ . See the Supporting Information for experimental and structural details.

A combination of X-ray crystallography and DFT studies has led to the following striking conclusions. Copper corroles are inherently nonplanar, *even in the absence of sterically hindered substituents*. In contrast, cobalt(III) corroles are planar, *even if they are highly sterically hindered*. These counterintuitive findings are unprecedented for metallocorroles as well as for metalloporphyrins. As we will discuss in detail below, the inherent nonplanarity of copper corroles is driven by a specific copper–corrole orbital interaction. Given that copper corroles are among the most readily accessible metallocorroles,<sup>13</sup> the findings reported herein are almost certain to prove relevant to a broad cross section of corrole chemistry.

## Experimental Section

Unless otherwise mentioned, all reagents and solvents were used as received. Silica gel 60 (0.04–0.063-mm particle size, 230–240 mesh, Merck) was used for flash chromatography. Silica gel 60 (20 × 20 cm, 0.5-mm thickness, Merck) was also used for preparative thin-layer chromatography for further purification. All samples for NMR analysis were prepared in 5-mm NMR tubes using CDCl<sub>3</sub>. <sup>1</sup>H NMR spectra are recorded with a Varian 400 MHz spectrometer at 298 K and referenced to residual CHCl<sub>3</sub> (δ = 7.26 ppm). UV–vis spectra were recorded with an HP 8453 spectrometer in CH<sub>2</sub>Cl<sub>2</sub>. Elemental analyses were obtained from Atlantic Microlab, Inc., Norcross, GA.

**General Procedure for the Preparation of the Free Base *trans*-A<sub>2</sub>B-triarylcorroles.** To the appropriate aldehyde (0.5 mmol) and aryldipyrromethane (1 mmol), dissolved in 100 mL of MeOH, was added 100 mL of H<sub>2</sub>O and 2.5 mL of 37% HCl, and the reaction mixture was stirred at room temperature for 1 h.<sup>1c</sup> The mixture was then extracted with CHCl<sub>3</sub>; the organic layer was washed twice with distilled H<sub>2</sub>O, dried with Na<sub>2</sub>SO<sub>4</sub>, filtered, and diluted to 250 mL with CHCl<sub>3</sub>. *p*-Chloranil (369 mg) was added, and the mixture was stirred at room temperature for 2 h. The mixture was then evaporated to dryness in a rotary evaporator, and the crude material was subjected to flash chromatography (silica gel, 1:1 *n*-hexane/dichloromethane). All fractions containing corroles were combined and evaporated. Subsequent column chromatography (silica gel, 3:2 hexane/dichloromethane) and crystallization (CH<sub>2</sub>Cl<sub>2</sub>/*n*-hexane) afforded the pure free-base corrole.

**Free Base 10-(*p*-Methoxyphenyl)-5,15-diphenylcorrole.** Yield: 165 mg (59.1%). <sup>1</sup>H NMR (CDCl<sub>3</sub>): δ 8.93 (s, 2H, β-pyrrolic), 8.88 (s, 2H, β-pyrrolic), 8.56 (br s, 4H, β-pyrrolic) 8.36 (br s, 4H, 5,15-*o*-phenyl), 8.08 (br s, 2H, 10-*o*- or *m*-phenyl), 7.82 (br s, 4H, 5,15-*m*-phenyl), 7.73 (br s, 2H, *p*-phenyl), 7.31 (br s, 2H, 10-*m*- or *o*-phenyl), 4.1 (br s, 3H, 10-*p*-OCH<sub>3</sub>). MS (MALDI-TOF, major isotopomer): M<sup>+</sup> 556.15 (exp), 556.22 (calcd).

**Free Base 10-(*p*-Methoxyphenyl)-5,15-bis[*p*-(trifluoromethyl)phenyl]corrole.** Yield: 170 mg (49%). <sup>1</sup>H NMR (CDCl<sub>3</sub>): δ 8.82 (s, 4H, β-pyrrolic), 8.61 (s, 2H, β-pyrrolic), 8.46 (br s, 6H, β-pyrrolic and 5,15-*o*- or *m*-phenyl), 8.1 (br s, 4H, 5,15-*m*- or *o*-phenyl), 8.05 (br s, 2H, 10-*o*- or *m*-phenyl), 7.31 (br s, 2H, 10-*m*- or *o*-phenyl), 4.10 (s, 3H, 10-*p*-OCH<sub>3</sub>). MS (MALDI-TOF, major isotopomer): M<sup>+</sup> 692.35 (exp), 692.20 (calcd).

**General Procedure for Copper Insertion.** The copper corrole complexes were synthesized as reported by Wasbotten et al.<sup>8</sup>

**Copper 10-(*p*-Methoxyphenyl)-5,15-diphenylcorrole.** Yield: 83%. UV–vis [ $\lambda_{\text{max}}$ , nm ( $\epsilon \times 10^{-4}$ , M<sup>-1</sup> cm<sup>-1</sup>): 408 (4.87), 524 (0.64)]. <sup>1</sup>H NMR (CDCl<sub>3</sub>): δ 7.87 (d, *J* = 3.2 Hz, 2H, β-pyrrolic), 7.78 (d, *J* = 7.2 Hz, 4H, 5,15-*o*-phenyl), 7.66 (d, *J* = 4.4 Hz, 2H, β-pyrrolic),

7.63 (d, *J* = 8.8 Hz, 2H, 10-*o*- or *m*-phenyl), 7.59 (t, *J* = 7.4 Hz, 2H, 5,15-*p*-phenyl), 7.49 (t, *J* = 7.4 Hz, 4H, 5,15-*m*-phenyl), 7.35 (d, *J* = 4.4 Hz, 2H, β-pyrrolic), 7.31 (d, *J* = 4.8 Hz, 2H, β-pyrrolic), 6.99 (d, *J* = 8.4 Hz, 2H, 10-*m*- or *o*-phenyl), 3.91 (s, 3H, 10-*p*-OCH<sub>3</sub>). MS (MALDI-TOF, major isotopomer): M<sup>+</sup> 616.18 (exp), 616.13 (calcd). Elem anal. Calcd for C<sub>38</sub>H<sub>25</sub>N<sub>4</sub>O<sub>2</sub>Cu: C, 73.95; H, 4.08; N, 9.08. Found: C, 73.54; H, 4.00; N, 8.73.

**Copper 10-(*p*-Methoxyphenyl)-5,15-bis[*p*-(trifluoromethyl)phenyl]corrole.** Yield: 85%. UV–vis [ $\lambda_{\text{max}}$ , nm ( $\epsilon \times 10^{-4}$ , M<sup>-1</sup> cm<sup>-1</sup>): 407 (5.54), 434 (4.06), 526 (0.73)]. <sup>1</sup>H NMR (CDCl<sub>3</sub>): δ 7.86 (d, *J* = 8.4 Hz, 4H, 5,15-*o*- or *m*-phenyl), 7.85 (d, *J* = 4.4 Hz, 2H, β-pyrrolic), 7.75 (d, *J* = 8.4 Hz, 4H, 5,15-*m*- or *o*-phenyl), 7.59 (d, *J* = 4.4 Hz, 2H, β-pyrrolic), 7.58 (d, *J* = 8.4 Hz, 2H, 10-*o*- or *m*-phenyl), 7.32 (d, *J* = 4.8 Hz, 2H, β-pyrrolic), 7.29 (d, *J* = 4.0 Hz, 2H, β-pyrrolic), 6.99 (d, *J* = 8.8 Hz, 2H, 10-*m*- or *o*-phenyl), 3.92 (s, 3H, 10-*p*-OCH<sub>3</sub>). MS (MALDI-TOF, major isotopomer): M<sup>+</sup> 752.27 (exp), 752.10 (calcd). Elem anal. Calcd for C<sub>40</sub>H<sub>23</sub>F<sub>6</sub>N<sub>4</sub>O<sub>2</sub>Cu: C, 63.79; H, 3.08; N, 7.44. Found: C, 63.88; H, 3.04; N, 7.46.

**Crystallization.** X-ray-quality crystals of the copper corrole complexes were obtained from *n*-hexane/dichloromethane. The copper complexes were fully dissolved in a minimum volume of dichloromethane, and to the clear solution was added a 3-fold excess of *n*-hexane. The Erlenmeyer flask containing this mixture was covered with Parafilm, which was then pierced with a needle to allow slow evaporation, and left to stand for 1 week. The supernatant liquid was then decanted off, and the crystals, washed with pure *n*-hexane, were of X-ray quality.

**DFT Calculations.**<sup>14</sup> In general, all calculations were carried out with the OLYP<sup>15–17</sup> exchange-correlation functional and all-electron STO-TZP basis sets, as implemented in the ADF2007<sup>18</sup> program system. Throughout we used a suitably fine grid for numerical integration of the matrix elements, and tight convergence criteria for both self-consistent field and geometry iterations were employed. Although DFT, regardless of the functional, normally performs very well for late-transition-metal porphyrinoids,<sup>19,20</sup> we checked selected results with B3LYP<sup>21,16</sup>/6-311G(d,p) calculations with the Gaussian03<sup>22</sup> software. The B3LYP-optimized geometries proved to be nearly identical with those obtained with OLYP. However, unlike OLYP, B3LYP resulted in a degree of spin-symmetry-breaking, i.e., a spatial separation of  $\alpha$  and  $\beta$  spin densities.

(14) The DFT (OLYP) calculations were carried out with the ADF2007 program system using the methods described in: Velde, G. T.; Bickelhaupt, F. M.; Baerends, E. J.; Guerra, C. F.; Van Gisbergen, S. J. A.; Snijders, J. G.; Ziegler, T. *J. Comput. Chem.* **2001**, *22*, 931–967.

(15) The OPTX exchange functional: Handy, N. C.; Cohen, A. *J. Mol. Phys.* **2001**, *99*, 403–412.

(16) The LYP correlation functional: Lee, C.; Yang, W.; Parr, R. G. *Phys. Rev.* **1988**, *B37*, 785–789.

(17) For transition-metal systems, the OPTX-based functionals OLYP and OPBE have often been found to perform better than classic pure functionals and sometimes even better than B3LYP: (a) Conradie, J.; Ghosh, A. *J. Chem. Theory Comput.* **2007**, *3*, 689–702. (b) Conradie, J.; Ghosh, A. *J. Phys. Chem. B* **2007**, *111*, 12621–12624. (c) Swart, M. *J. Chem. Theory Comput.* **2008**, *4*, 2057–2066.

(18) The ADF program system was obtained from Scientific Computing and Modeling, Amsterdam, The Netherlands (<http://www.scm.com/>). For a description of the methods used in ADF, see: Velde, G. T.; Bickelhaupt, F. M.; Baerends, E. J.; Guerra, C. F.; Van Gisbergen, S. J. A.; Snijders, J. G.; Ziegler, T. *J. Comput. Chem.* **2001**, *22*, 931–967.

(19) For a relevant recent study on nickel hydrophorphyrins, see: Ryeng, H.; Gonzalez, E.; Ghosh, A. *J. Phys. Chem. B* **2008**, *112*, 15158–15173. The situation is quite different for middle-transition-metal porphyrins, notably hemes, where different functionals often give widely divergent results.

(20) For comparative studies of different exchange-correlation functionals for transition-metal systems and for calibration against high-level ab initio results, see: (a) Ghosh, A.; Taylor, P. R. *Curr. Opin. Chem. Biol.* **2003**, *7*, 113–124. (b) Ghosh, A. *J. Biol. Inorg. Chem.* **2006**, *11*, 712–724.

(21) (a) Becke, A. D. *Phys. Rev. A* **1988**, *38*, 3098–3100. (b) Becke, A. D. *J. Chem. Phys.* **1993**, *98*, 1372. (c) Becke, A. D. *J. Chem. Phys.* **1993**, *98*, 5648.

(22) Frisch, M. J.; et al. *Gaussian03*; Gaussian, Inc.: Wallingford, CT, **2004**.

(13) Copper corroles are useful starting materials for free bases and metallocorroles that are otherwise inaccessible. Capar, C.; Thomas, K. E.; Ghosh, A. *J. Porphyrins Phthalocyanines* **2008**, *12*, 964–967.

## Results and Discussion

(a) **Copper Corrole Crystal Structures.** Both crystal structures (Figure 1) exhibit Cu–N distances averaging around 1.9 Å, which is typical for copper(III) complexes. We will see, however, that a copper(III) description may not be appropriate for these complexes. The novel feature of the crystal structures is that the corrole macrocycle is significantly saddled (i.e., the pyrrole rings are alternately tilted up and down). Saddling is not unprecedented for copper corroles,<sup>23</sup> but key examples have involved sterically hindered derivatives such as copper *meso*-tris(2,6-dichlorophenyl)corrole<sup>24</sup> and copper 2,3,7,8,12,13,17,18-octaethyl-5,15-diphenylcorrole.<sup>25</sup> The crystal structures shown in Figure 1 are unique examples of sterically *unhindered* metallocorroles that are significantly nonplanar. The unusual nature of these structures may be appreciated when one recalls that even highly hindered metallocorroles may be essentially planar, as is the case for low-spin cobalt(III)<sup>26</sup> and iridium(III)<sup>27</sup>  $\beta$ -octabromo-*meso*-triarylcorroles with amine or phosphine axial ligands.

(b) **DFT Saddling Potentials.** The surprising structural chemistry described above led us to consider copper-specific metal–ligand interactions that could possibly engender the saddled structures shown in Figure 1. To find out, we carried out DFT calculations on the copper and cobalt(III)-triphenylphosphine complexes of four different corrole ligands: unsubstituted corrole (C), *meso*-triphenylcorrole (TPC),  $\beta$ -octabromo-*meso*-triphenylcorrole (Br<sub>8</sub>TPC), and  $\beta$ -octakis(trifluoromethyl)-*meso*-triphenylcorrole {(CF<sub>3</sub>)<sub>8</sub>TPC}.<sup>10</sup> All molecular geometries were fully optimized (under a C<sub>2</sub> symmetry constraint), and saddling potentials were evaluated as a function of the C<sub>8</sub>–C<sub>9</sub>–C<sub>11</sub>–C<sub>12</sub> dihedral angle (denoted  $\chi$  in Figure 2). The results revealed a dramatic difference between the copper and cobalt energy landscapes. Thus, whereas the sterically uncrowded Cu(TPC) complex exhibits a fairly high degree of saddling ( $\chi > 40^\circ$ ), even the most hindered cobalt corroles exhibit nearly planar structures ( $\chi < 8^\circ$ ). These results strongly suggest (correctly, as it turns out) that copper-specific orbital interactions are responsible for the observed saddled geometries.<sup>28</sup>

Table 1 presents the symmetry-unique saddling dihedrals for the OLYP-optimized geometries of the Cu(TPC) derivatives studied. The corresponding experimental values, averaged over the two crystal structures, are also shown for comparison. DFT (OLYP/STO-TZP) and

**Table 1.** Symmetry-Unique Saddling Dihedrals (deg) from OLYP/STO-TZP-Optimized Geometries

	C <sub>3</sub> –C <sub>4</sub> –C <sub>6</sub> –C <sub>7</sub>	C <sub>8</sub> –C <sub>9</sub> –C <sub>11</sub> –C <sub>12</sub>	C <sub>2</sub> –C <sub>1</sub> –C <sub>19</sub> –C <sub>18</sub>
Cu(TPC)	48	44	25
Cu(Br <sub>8</sub> TPC)	69	67	44
Cu[(CF <sub>3</sub> ) <sub>8</sub> TPC]	99	98	74
exp (mean)	51	44	29

experiment are clearly in good accord as far as macrocycle nonplanarity is concerned;<sup>19</sup> other geometry parameters such as the short Cu–N distances of about 1.9 Å are also well-reproduced in the calculations. Unfortunately, although we have synthesized Cu(Br<sub>8</sub>TPC) and Cu[(CF<sub>3</sub>)<sub>8</sub>TPC],<sup>8,10</sup> we have not been able to obtain their crystal structures, so we are unable to experimentally confirm the most dramatic saddling deformations predicted below.

(c) **Key Saddling-Inducing Orbital Interaction.** In porphyrins, saddling switches on the metal(d<sub>x<sup>2</sup>–y<sup>2</sup></sub>)–porphyrin (a<sub>2u</sub> HOMO) interaction.<sup>29</sup> An exactly analogous scenario may be envisioned for metallocorroles, whose ring HOMOs closely resemble porphyrin HOMOs in shape.<sup>30</sup> An examination of the HOMO of any copper corrole readily confirms this hypothesis, as illustrated in Figure 3 by the HOMO of Cu(TPC). Saddling allows a good deal (about 50%) of electron density from the b-symmetry (with reference to the C<sub>2</sub> point group)  $\pi$ -HOMO (the analogue of the porphyrin a<sub>2u</sub> HOMO) to flow into the space of the Cu d<sub>x<sup>2</sup>–y<sup>2</sup></sub> orbital. In other words, the copper center is not quite trivalent, despite the short Cu–N distance, but has substantial copper(II) character. Light-heartedly put, copper corroles are literally saddled with a noninnocent ligand.

How much is the Cu(d<sub>x<sup>2</sup>–y<sup>2</sup></sub>)–corrole (HOMO) interaction worth in energy terms? The ferro- ( $S = 1$ ) and antiferromagnetically coupled ( $S = 0$ ) Cu<sup>II</sup>–corrole<sup>2–</sup> states of Cu(TPC) differ by about 0.1 eV (OLYP/STO-TZP), which is essentially the same as that in early calculations of the singlet–triplet splittings for a planar conformation of copper corrole.<sup>9,29</sup> Saddling is typically a soft deformation, and this amount of energy is adequate to account for the saddling deformations observed for the substituted Cu(TPC) derivatives reported in this paper.

Variable-temperature NMR spectroscopy has long shown the existence of thermally accessible paramagnetic states for copper corroles.<sup>9</sup> For the present complexes as well, certain  $\beta$  protons in the <sup>1</sup>H NMR spectra exhibit increasingly broad signals with increasing temperature, as expected (as shown in the Supporting Information). NMR spectroscopy, along with DFT and multiconfigurational ab initio calculations, has also indicated noninnocent electronic structures for chloroiron corrole derivatives.<sup>31</sup> Ligand

(23) Brückner, C.; Brinas, R. P.; Bauer, J. A. K. *Inorg. Chem.* **2003**, *42*, 4495–4497.

(24) Luobeznova, I.; Simkhovich, L.; Goldberg, I.; Gross, Z. *Eur. J. Inorg. Chem.* **2004**, 1724–1732.

(25) Bröring, M.; Bregier, F.; Tejero, E. C.; Hell, C.; Holthausen, M. C. *Angew. Chem., Int. Ed.* **2007**, *46*, 445–448.

(26) Paolesse, R.; Nardis, S.; Sagone, F.; Khoury, R. G. *J. Org. Chem.* **2001**, *66*, 550–556.

(27) Palmer, J. H.; Day, M. W.; Wilson, A. D.; Henling, L. M.; Gross, Z.; Gray, H. B. *J. Am. Chem. Soc.* **2008**, *130*, 7786–7787.

(28) Given that copper corroles are four-coordinate and Co<sup>III</sup>PPh<sub>3</sub> corroles are five-coordinate, the question might be raised as to whether PPh<sub>3</sub> exerts a planarizing influence in the latter case. To address this question, we also calculated the saddling potentials for four-coordinate cobalt(III) corroles. For unsubstituted corrole and TPC,  $\chi < 10^\circ$  for both the  $S = 0$  and 1 spin states of the four-coordinate cobalt(III) complex. Even for Co<sup>III</sup>(Br<sub>8</sub>TPC), the saddling dihedral was found to be only about 16°. Thus, the triphenylphosphine ligand does not play a significant role in conferring a planar geometry on cobalt corroles.

(29) For reviews on nonplanar porphyrins, see: (a) Senge, M. *Chem. Commun.* **2006**, 243–256. (b) Shelnutz, J. A.; Song, X. Z.; Ma, J. G.; Jia, S. L.; Jentzen, W.; Medforth, C. J. *Chem. Soc. Rev.* **1998**, *27*, 31–41.

(30) Ghosh, A.; Wondimagegn, T.; Parusel, A. B. *J. Am. Chem. Soc.* **2000**, *122*, 5100–5104.

(31) (a) Cai, S.; Walker, F. A.; Licoccia, S. *Inorg. Chem.* **2000**, *39*, 3466–3478. (b) Zakhariyeva, O.; Schunemann, V.; Gerdan, M.; Licoccia, S.; Cai, S.; Walker, F. A.; Trautwein, A. X. *J. Am. Chem. Soc.* **2002**, *124*, 6636–6648. (c) Walker, F. A.; Licoccia, S.; Paolesse, R. *J. Inorg. Biochem.* **2006**, *100*, 810–837. (d) Gross, Z.; Gray, H. B. *Comments Inorg. Chem.* **2006**, *27*, 61–72. (e) Roos, B. O.; Veryazov, V.; Conradie, J.; Taylor, P. R.; Ghosh, A. *J. Phys. Chem.* **2008**, *112*, 14099–14102. (f) Ye, S.; Tuttle, T.; Bill, E.; Simkhovich, L.; Gross, Z.; Thiel, W.; Neese, F. *Chem. Eur. J.* **2008**, *14*, 10839–10851.

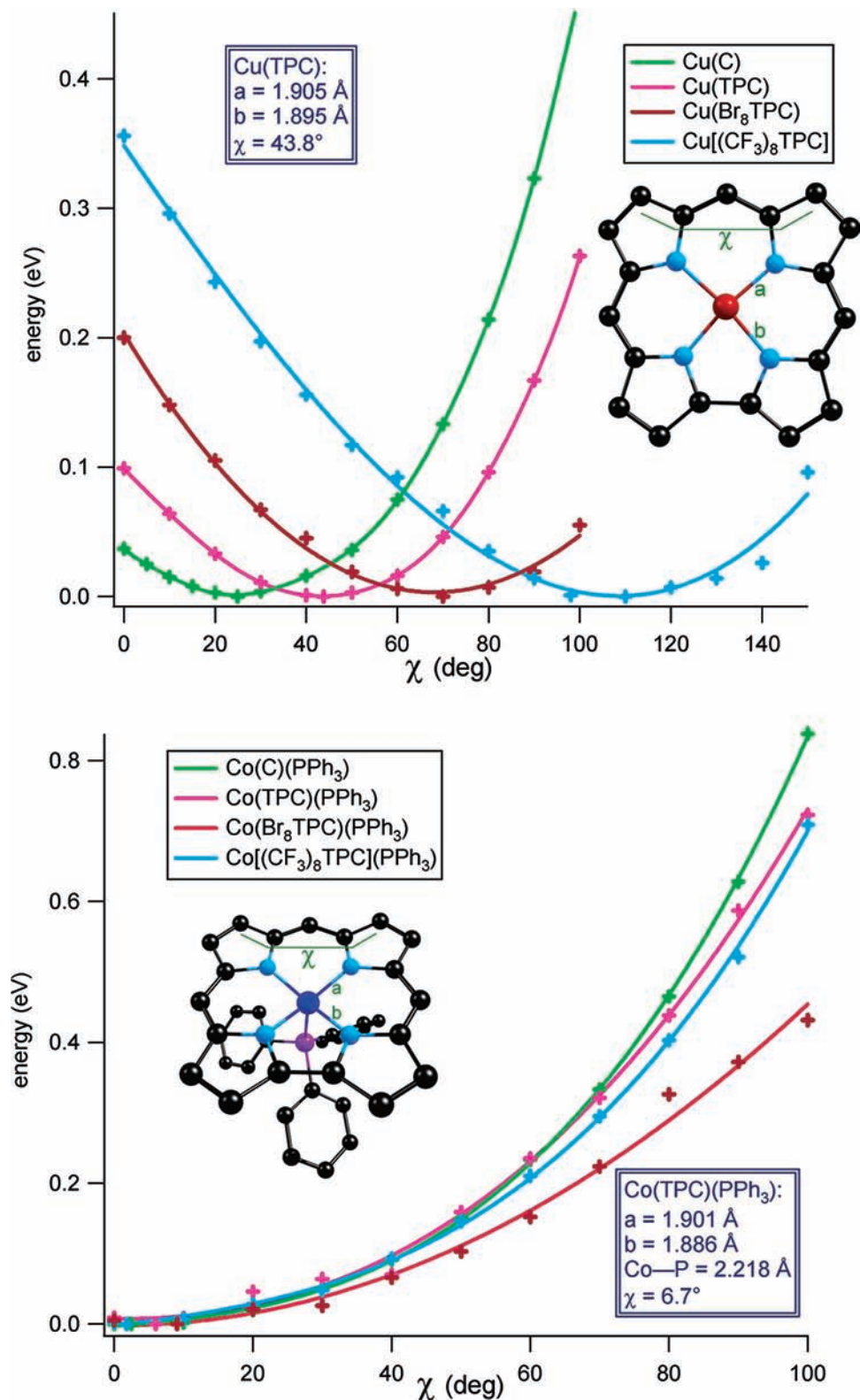


**Figure 2.** OLYP/STO-TZP saddling potentials for Cu (top) and Co(PPh<sub>3</sub>) (bottom) corrole derivatives as a function of the C<sub>8</sub>–C<sub>9</sub>–C<sub>11</sub>–C<sub>12</sub> dihedral angle ( $\chi$ ). Key geometry parameters for the TPC derivatives are shown in the blue insets.

noninnocence thus is ubiquitous (although not absolutely universal) in metallocorrole chemistry.

**(d) Comparison with Porphyrin Chemistry.** The results presented above have proved that a purely electronic effect, i.e., a specific metal–ligand orbital interaction, may provide a sufficient driving force to engender sig-

nificant buckling of the corrole  $\pi$  system. We suggest that the phenomena reported here are unique not only in metallocorrole chemistry but also in the larger context of porphyrin chemistry.

The metal( $d_{x^2-y^2}$ )–porphyrin( $a_{2u}$ ) orbital interaction is certainly well-precedented in porphyrin chemistry.

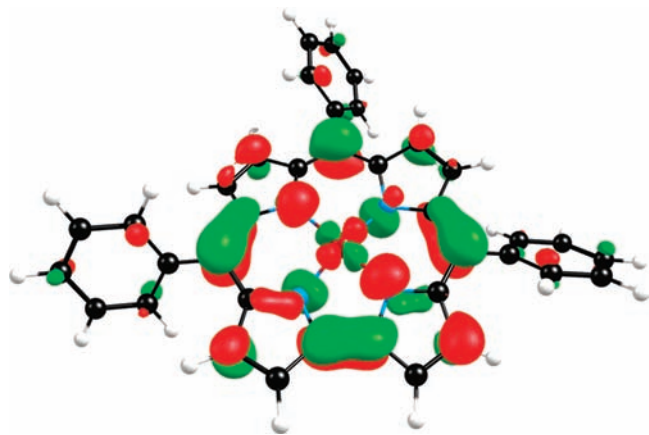


**Figure 3.** Spin-restricted OLYP/STO-TZP HOMO of Cu(TPC). The contour value has been set to  $0.05 \text{ e } \text{\AA}^{-3}$ .

It explains, for instance, why saddled copper porphyrins are more easily oxidized relative to analogous saddled nickel porphyrins.<sup>32</sup> The same orbital interaction also accounts for the diamagnetism of saddled copper porphyrin  $\pi$ -cation radical derivatives.<sup>33,34</sup> However, in none

(32) Ghosh, A.; Halvorsen, I.; Nilsen, H. J.; Steene, E.; Wondimagegn, T.; Lie, E.; van Caemelbecke, E.; Guo, N.; Ou, Z.; Kadish, K. M. *J. Phys. Chem. B* **2001**, *105*, 8120–8124.

(33) Renner, M. W.; Barkigia, K. M.; Zhang, Y.; Medforth, C. J.; Smith, K. M.; Fajer, J. *J. Am. Chem. Soc.* **1994**, *116*, 8582–8592.

(34) Renner, M. W.; Barkigia, K. M.; Fajer, J. *Inorg. Chim. Acta* **1997**, *263*, 181–187.

of these cases is the saddling a *result* of the orbital interaction. For metalloporphyrins, this orbital interaction is undoubtedly strengthened by saddling; however, without exception, the saddling arises primarily as a result of peripheral steric crowding. The inherent (i.e., metal–ligand orbital interaction-driven) saddling of copper corroles thus is fundamentally novel.

### Concluding Remarks

Crystallographic and DFT studies have led to the uncovering of a remarkable facet of metallocorrole structural chemistry; viz., copper corroles are inherently saddled (and indeed chiral), even in the absence of sterically hindered substituents. In contrast, low-spin cobalt(III) corroles are planar, even in the presence of a great deal of peripheral steric crowding. This suggests that, barring specific metal–ligand orbital interactions, metallocorroles are significantly less prone to nonplanar distortions, relative to metalloporphyrins. Corroles, however, are more prone to adopt noninnocent electronic structures than porphyrins, and in the case of copper corroles, this provides a sufficient driving force to bring about saddling.

**Acknowledgment.** This work was supported by the Research Council of Norway.

**Supporting Information Available:** Spectra and X-ray analyses, OLYP/TZP-optimized geometries, and X-ray crystallographic data in CIF format. This material is available free of charge via the Internet at <http://pubs.acs.org>.